Application of Sentinel-2A data for pasture biomass monitoring using a physically based radiative transfer model

Remote Sensing of Environment 218 (2018) 207–220

Contents lists available at ScienceDirect

Remote Sensing of Environment

journal homepage: www.elsevier.com/locate/rse

Application of Sentinel-2A data for pasture biomass monitoring using a physically based radiative transfer model

S.M. Punalekar[a], A. Verhoef[a,*], T.L. Quaife[b], D. Humphries[c], L. Bermingham[d], C.K. Reynolds[c]

[a] Dept. of Geography and Environmental Science, University of Reading, Reading RG6 6UR, UK
[b] National Centre for Earth Observation, Dept. of Meteorology, University of Reading, Reading RG6 6BB, UK
[c] Centre for Dairy Research, School of Agriculture, Policy and Development, The University of Reading, Reading RG6 6AR, UK
[d] Rezatec, Harwell Campus, Didcot OX11 0RA, UK

ARTICLE INFO

Keywords:
Sentinel 2A
Leaf Area Index
Pasture
Grassland
Radiative transfer
Model inversion
Satellite retrieval

ABSTRACT

A large proportion of the global land surface is covered by pasture. The advent of the Sentinel satellites program provides free datasets with good spatiotemporal resolution that can be a valuable source of information for monitoring pasture resources. We combined optical remote sensing data (proximal hyperspectral and Sentinel 2A) with a radiative transfer model (PROSAIL) to estimate leaf Area Index (*LAI*), and biomass, in a dairy farming context. Three sites in Southern England were used: two pasture farms that differed in pasture type and management, and a set of small agronomy trial plots with different mixtures of grasses, legumes and herbs, as well as pure perennial ryegrass. The proximal and satellite spectral data were used to retrieve *LAI via* PROSAIL model inversion, which were compared against field observations of *LAI*. The potential of bands of Sentinel 2A that corresponded with a 10 m resolution was studied by convolving narrow spectral bands (from a handheld hyperspectral sensor) into Sentinel 2A bands (10 m). Retrieved *LAI*, using these spectrally resampled S2A data, compared well with measured *LAI*, for all sites, even for those with mixed species cover (although retrieved *LAI* was somewhat overestimated for pasture mixtures with high *LAI*). This proved the suitability of 10 m Sentinel 2A spectral bands for capturing *LAI* dynamics for different types of pastures. We also found that inclusion of 20 m bands in the inversion scheme did not lead to any further improvement in retrieved *LAI*. Sentinel 2A image based retrieval yielded good agreement with *LAI* measurements obtained for a typical perennial ryegrass based pasture farm. *LAI* retrieved in this way was used to create biomass maps (that correspond to indirect biomass measurements by Rising Plate Meter (RPM)), for mixed-species paddocks for a farm for which limited field data were available. These maps compared moderately well with farmer-collected RPM measurements for this farm. We propose that estimates of paddock-averaged and within-paddock variability of biomass are more reliably obtained from a combined Sentinel 2A-PROSAIL approach, rather than by manual RPM measurements. The physically based radiative transfer model inversion approach outperformed the Normalized Difference Vegetation Index based retrieval method, and does not require site specific calibrations of the inversion scheme.

1. Introduction

Grasslands ecosystems, including managed pastures, are one of the largest ecosystems of the world; currently 26% of global land area and 70% of total agricultural area is under pasture and fodder crops (http://www.fao.org). Grazing ruminants convert grass and other fibrous forage materials into milk and meat for human consumption; ruminant production represents a key agricultural enterprise, particularly in the more developed countries (Thornton, 2010). Pasture management, together with local weather conditions, will affect productivity and pasture quality and hence farm output. Thus, there is a need for regular herbage monitoring and prediction of pasture growth rates and quality indicators. Such information assists the efficient utilization of pastures by avoiding overgrazing, providing guidance with regards to food supplement decisions or alerting farmers to wastage during periods of surplus pasture availability. Dairy farmers practicing rotational grazing systems generally keep track of pasture productivity through 'field walking'. This involves regular assessments of biomass, either visually by a simple estimation of the grass height, or by using a more technological approach, such as a 'rising plate meter' (RPM) which measures both the height and density of the grass sward. The equations required to convert compressed pasture height to biomass can vary per

* Corresponding author.
E-mail address: a.verhoef@reading.ac.uk (A. Verhoef).

https://doi.org/10.1016/j.rse.2018.09.028
Received 13 October 2017; Received in revised form 4 September 2018; Accepted 30 September 2018

country, per year and per season and also as per type of pasture (Bransby et al., 1977; Huillier and Thomson, 1988; Ferraro et al., 2012; Somasiri et al., 2014). Therefore accurate 'on farm' prediction of biomass requires that the correct regional, seasonal and pasture specific conversion equation is used. However, for practical on-farm use operators of RPM systems tend to use a single equation (with constant coefficients) for the entire grazing season. This approach can lead to inaccurate prediction of the available biomass (Nakagami and Itano, 2013) with a consequential reduction in utilization efficiency.

Furthermore, regular pasture walking can be time consuming and labor intensive. If not performed following key guidelines, traditionally used methods (such as RPM monitoring, visual appraisal, pastures sticks and boot height) for pasture biomass quantification can produce inaccurate estimates of sward biomass. This is a consequence of the large within-field spatial variability of grass growth (generally associated with low stocking rate), so that the recommended minimum of 50–80 measurements per field (Thomson et al., 1997) may not be enough to enable accurate estimation of average grass biomass at any moment in time. Profit margins in pasture based farming are small and automatically monitoring grass growth to maximise production could make a real difference to farmers by aiding in increasing the efficiency of use of the cheapest feed input available (*i.e.*, grass).

If grass quantity and quality can be determined from space (*i.e. via* satellite), with suitable accuracy and spatial/temporal resolution, this would open up a host of possibilities for more efficient pasture management and more profitable pasture farming. Similar to ground based methods, remote sensing based pasture monitoring is also prone to errors due to a range of factors such as sensor noise, radiometric as well as geometric corrections, errors associated with atmospheric corrections, and inadequate BRDF models (Fernandes et al., 2014). Nevertheless, despite these limitations satellite images have significant potential due to their spatiotemporal coverage. The recent European Space Agency satellite program Sentinel 2 comprises two satellites that ensure continuity for SPOT and LANDSAT programs and provide images with as fine as 10 m pixel size every five days (depending on latitude). These freely available data are ideal for monitoring pasture biomass availability on pasture farms and offer the opportunity to develop robust algorithms to exploit their potential in efficient and cost effective pasture monitoring.

The use of remote sensing for monitoring and prediction of arable crop growth (with an emphasis on optical remote sensing) is already well established (Bégué et al., 2018; Ozdogan et al., 2010). However, the same is not true for forage crops used for grazing or silage in animal and dairy production systems. Remote monitoring of grass production is difficult due to the fact that intensively grazed pastures are very dynamic systems and grass crops need to be maintained carefully at optimum height to avoid over and under-utilization of pastures. Hence for intensively managed grazing pastures interpretation of remote sensing data is difficult without detailed knowledge of farming operations (Edirisinghe et al., 2012).

Despite these limitations there have been some notable research efforts that investigated applications of remote sensing data for regular pasture monitoring. Hill et al. (2004) used AVHRR based normalized difference vegetation index (*NDVI*) time series to produce maps of pasture growth rate in Western Australia. Following these efforts scientists from Australia and New Zealand discussed applications of MODIS, Landsat and SPOT for operational monitoring of grazing paddocks (Eastwood et al., 2009; Mata et al., 2011; Edirisinghe et al., 2012), mainly under the framework of the 'Pasture from Space' program. Di Bella et al. (2004) studied 13 forage regions in France, looking at the spatial and seasonal variability in grassland productivity in relation to drought. They used images from (SPOT) 4-VEGETATION to forecast variables related to grass production that were compared to the STICS-Prairie simulation model. Schino et al. (2003) demonstrated application of Landsat *NDVI* for monitoring biomass in Alpine pastures in Italy. Researchers have also investigated hyperspectral data and narrow band indices for pasture characterization in terms of biomass (Boschetti et al., 2007) as well as pasture quality parameters such as nutrient content and dead biomass content (Mutanga and Skidmore, 2004; Pullanagari et al., 2016, 2017). However, remote sensing of pastures has mainly followed spectral index based methods that are inherently empirical in nature (Schino et al., 2003; Eastwood et al., 2009; Fava et al., 2009; Edirisinghe et al., 2012). Furthermore, hyperspectral data are costly and field-scale relationships based on *in-situ* hyperspectral data have rarely been up-scaled and tested at the satellite image level.

Ali et al. (2016) presented a review of the current status of grassland monitoring/observation methods and applications based on satellite remote sensing data, and related technological and methodological developments, to retrieve grassland information. They noted that the retrieval of grassland biophysical parameters is moving from standard regression analysis to more mechanistic and hence more robust modeling approaches, driven by satellite data. Radiative transfer model inversion based retrieval schemes have been widely studied at field, regional and global scales (Dorigo et al., 2007; Frederic and Buis, 2008; Verrelst et al., 2015). Recent developments for promoting process based, and hence more adaptive inversion schemes for biophysical retrievals, include hybrid methods coupling model inversion with vegetation index based relationships for quick regional scale mapping (Dorigo et al., 2009; Houborg et al., 2007), combination of radiative transfer simulations for training artificial neural nets and kernel based algorithms (Doktor et al., 2014; Verrelst et al., 2015; Vohland et al., 2010), and application of prior information or reflectance of neighbouring pixels or land cover classes to constrain solutions (Atzberger and Richter, 2012). However, despite these advancements in the biophysical parameter retrievals, the emphasis is still on statistical models for remote sensing based monitoring of grasslands (Jin et al., 2014; Song et al., 2014; Zhao et al., 2014; Li et al., 2016; Meng et al., 2017; Schucknecht et al., 2017). Considering the limitations of these empirical methods (Atzberger et al., 2011) and to promote radiative transfer model based approaches for operational pasture monitoring systems, new datasets such as Sentinel 2 have to be tested over a variety of pasture types and management operations. The Sentinel 2 satellite with high revisit frequency and good spatial resolution offers opportunity to develop operational systems for pasture monitoring with data being available within a couple of days of acquisition. These systems should be less dependent on site specific calibrations.

As pointed out by Darvishzadeh et al. (2011, 2008) radiative transfer models have seldom been applied for studying heterogeneous grassland canopies. Using field and airborne hyperspectral data these authors explored the potential of radiative transfer modeling to predict *LAI* in heterogeneous Mediterranean grassland. We investigate whether multispectral Sentinel 2 data can be equally useful for inversion of radiative transfer model PROSAIL (Jacquemoud et al., 2009), as an alternative to widely used empirical models to capture changes in pasture canopy in terms of Leaf Area Index (*LAI*). This was done by development of robust algorithms that can be applied over a variety of pasture types and throughout the entire growing season, with minimum data requirement for calibration. The present study discusses model verification results over three sites differing in pasture types and management regime.

The methods and results presented in this paper are contributing towards the operational system development by addressing the following research questions: (1) whether Sentinel 2A (S2A) optical data are able to capture spatio-temporal changes in pasture biomass, expressed as changes in *LAI*; (2) whether a Look Up Table (LUT) based radiative transfer model inversion algorithm is able to reliably estimate *LAI* over different types of pastures, *i.e.* perennial ryegrass and multiple

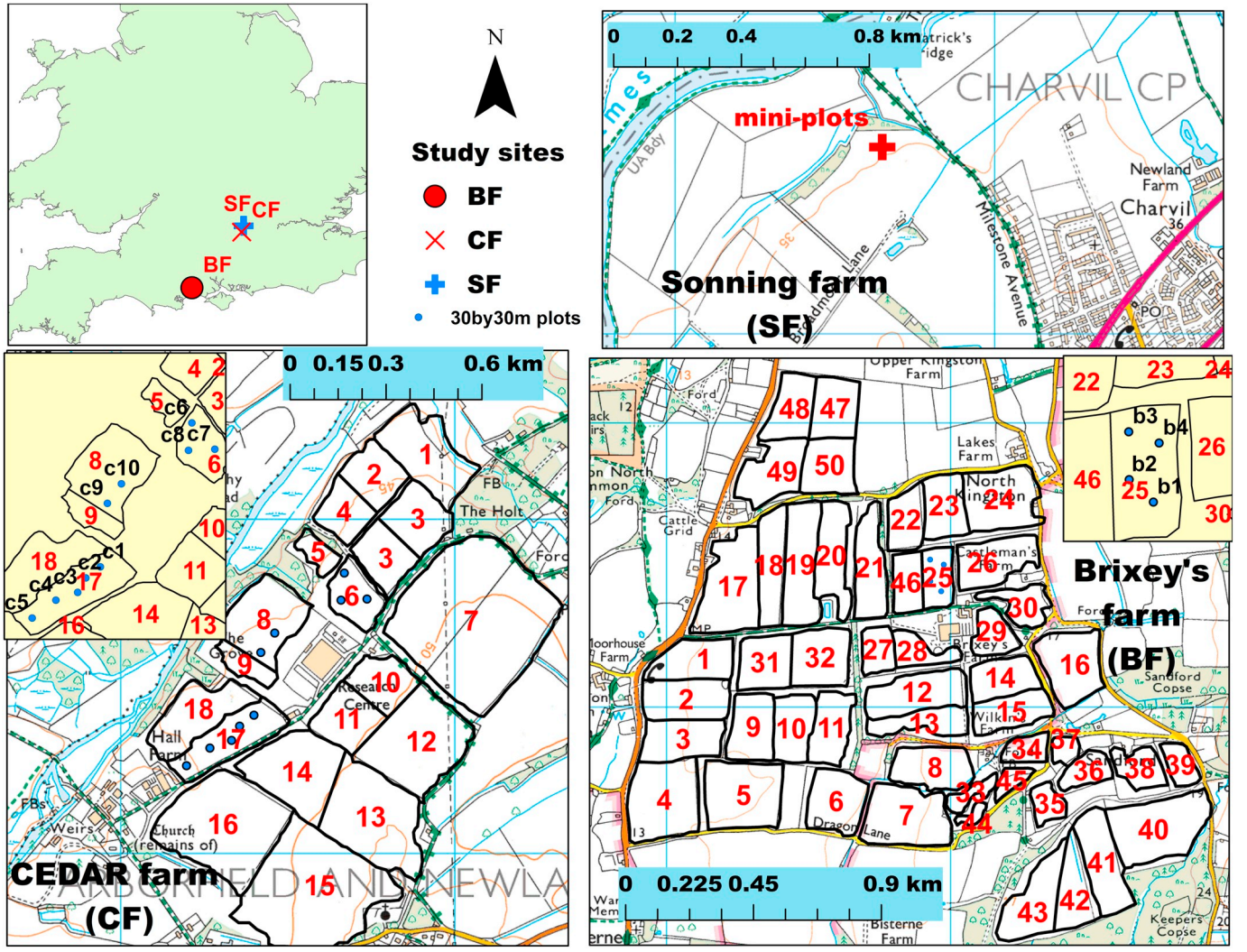

Fig. 1. Diagram showing location and details of three study sites against UK Ordnance Survey basemap (1:25000): Sonning farm, CEDAR Hall farm and Brixey's farm. In the case of CEDAR farm and Brixey's farm, farms have been divided in paddocks of different sizes. This figure also shows location of sampling plots on CEDAR farm and Brixey's farm.

species mixtures, as well as grazing paddocks and silage plots; (3) whether *LAI* maps can be usefully translated to RPM- equivalent biomass maps using a simple empirical approach. Finally, we also investigate how the LUT based algorithms perform in comparison to *NDVI* based ones.

2. Methodology

2.1. Study area, vegetation and management

Three sites in southern England were used for data-gathering and related analyses (Fig. 1). They differed in pasture type and management – typical perennial ryegrass paddocks at the Centre for Dairy Research (CEDAR) research platform; herbal, legume and grass mixed pasture paddocks at Brixey's Farm; and small agronomy trial plots with different mixtures of grass, legumes and herbs, as well as pure perennial ryegrass, located at Sonning farm. Both CEDAR farm and Sonning farm are part of the University of Reading agricultural research facilities, whereas Brixey's farm is a privately managed commercial dairy farm.

CEDAR farm (51.40°N, 0.91°W) is located near Arborfield, in the Loddon river catchment, about 3 km south of Reading (UK), see Fig. 1. Average elevation is ~45 m above mean sea level. The farm grazing platform comprises 140 ha, established on a clay capped gravel soil (prone to drought and waterlogging) and is divided in 19 paddocks of variable sizes that consist of predominantly perennial ryegrass leys under rotational grazing. Paddock 15 and 16 were under arable crops and on paddock 7 four different types of pastures were grown in ~200 m × 40 m strips. The composition of these types was similar to that of the agronomy trial plots at Sonning farm (described below). The commercial herd of 560 Holstein cows at CEDAR farm is managed as a continuous calving system, fed with two grazing groups: (i) Eighty cows that graze ryegrass paddocks in late lactation with milk yields < 25 l per day, and (ii) Sixty dry cows that are between lactations. The rest of the cows are indoor-housed. Grazing starts in late March and continues until late November and these two grazing groups are grazed separately on different paddocks.

Brixey's farm (50.82°N, 1.77°W), 3 km south of Ringwood, is river-terrace (interbedded clay, silts and sands) farmland located within the Avon river catchment, near the coast of southern England (Fig. 1). Average elevation is ~15 m and the total area is 167 ha, consisting of 50 paddocks. Brixey's farm concerns a mix of traditional perennial ryegrass leys and herbal leys, which include grasses (perennial ryegrass, timothy, cocksfoot and fescue) clover varieties (red, white, sweet, crimson, alsike), lucerne, sanfoin, chicory, plantain, yarrow and burnet. The grazing system is rotational by paddock with a 30 day rotation at the height of the season. A single herd of 500 Friesian Jersey crosses is

maintained in a spring block calving system. Paddocks are strip grazed wherein they are temporarily divided in strips with movable electric fence and with each paddock grazed intensively for 12 h to maintain a high stocking rate and avoid herbage wastage.

Sonning farm (51.47°N, 0.90°W) is located at about 4 km from Reading on mostly free-draining alluvial land on the south bank of the river Thames (Fig. 1). The soil has a sandy loam texture. Four different pasture types were grown in 4 m × 5 m sampling plots (with four replicates) that were monitored regularly: Perennial ryegrass (control), consisting of five varieties of ryegrass; 'smartgrass', consisting of three varieties of perennial ryegrass plus timothy, clover (red, white), chicory and ribgrass; 'biomix', consisting of Festulolium, perennial ryegrass, timothy, cocksfoot, meadow fescue, clover (alsike, red, white), Lucerne, yellow trefoil, chicory, and ribgrass; and 'herbal' consisting of Festulolium, cocksfoot, perennial ryegrass, timothy, meadow fescue, tall fescue, clover (red, white, alsike, sweet), birdsfoot trefoil, sainfoin, ribgrass, burnet, yarrow and sheep parsley. These plots were cut three times throughout the season, at peak growth stage, but before senescence.

2.2. Field data collection

Ten plots of 30 m × 30 m were demarcated on three paddocks at CEDAR farm – five on paddock number 17 (plots C1 to C5), two on paddock 8 (C9 and C10) and three on paddock 6 (C6–C8), see Fig. 1. This sampling plot size, equal to three times the pixel size, has been found appropriate when taking into account errors associated with geometric correction (Edirisinghe et al., 2012; Fernandes et al., 2014). Paddocks 6 and 17 (Fig. 1) were managed as grazed paddocks while paddock 8 was reserved for silage production until the middle of May 2017.

Table 1 summarises the data used in this paper for the different farms. For reasons related to farm management, it was decided to concentrate sampling efforts on paddock 17 (plots C1 to C5), and sample the other two paddocks only occasionally. Sampling days were chosen such that observations were available within 3 days after satellite overpass.

Field measurements included top of canopy hyperspectral reflectance, *LAI* and canopy height. In each 30 m × 30 m plot, measurements were taken along three transects, roughly in the centre of each 10 m × 30 m section of the plot. In each transect, measurements were taken every 3 m approximately, resulting generally in 27 to 30 observations per plot.

Spectra were collected using SVC HR2024i spectroradiometers (Spectra Vista Corporation, Poughkeepsie, USA) in dual field of view mode. A standard set-up for dual field of view and post-processing protocol was followed as described in Maclellan (2017). A fibre optics cable with 25° FOV, connected to the SVC, was used to measure spectra from approximately 1 m height above ground at nadir. The spectral data were post-processed using the NERC Field Spectroscopy Facility (http://fsf.nerc.ac.uk/) recommended protocol.

LAI was measured using a ceptometer (AccuPAR LP-80, Decagon Devices, Pullman, USA) and measurements took place on the same or subsequent day as the hyperspectral sampling. The instrument's leaf inclination factor was set to 1, assuming a spherical leaf angle distribution. Measurements were taken under stable sky conditions.

Canopy height was measured using a RPM (F200, Farmworks Ltd., New Zealand) and used to estimate biomass using an equation recommended by the UK Agriculture and Horticulture Development Board (https://ahdb.org.uk/) for UK pasture systems.

Field sampling was conducted at Brixey's farm on 10 Aug 2017 on four 30 m × 30 m plots, located in an herbal-grass mixture paddock. The exact same sampling protocol was followed as described above for CEDAR farm.

In the case of Sonning farm, 12–13 spectral reflectance measurements were done on each of the sixteen 4 m × 5 m mini-plots (see Section 2.1), followed by ten *LAI* measurements and ten RPM measurements.

Table 1
Farm-wise sampling dates and data used for calibration and verification of the retrieval scheme. ✓, X and NA denote presence, absence of data and 'not applicable', respectively.

Farms	Dates	*SVC data*	LAI	RPM	S2A images
CEDAR farm	5 Apr 2017	X	✓	✓	✓ (2 Apr 2017)
	11 Apr 2017	✓	✓	✓	X
	5 May 2017	✓	✓	✓	X
	25 May 2017	✓	✓	✓	✓ (22 May 2017)
	21 Jun 2017	✓	✓	✓	✓
	4 Aug 2017	✓	✓	✓	X
Sonning farm	28 Mar 2017	✓	✓	✓	NA
	21 Apr 2017	✓	✓	✓	NA
	3 May 2017	✓	✓	✓	NA
	1 Jun 2017	✓	✓	✓	NA
	12 Jun 2017	✓	✓	✓	NA
	22 Aug 2017	✓	✓	✓	NA
Brixey's farm	10 Aug 2017	✓	✓	✓	X
	21 Jul 2016[a]	X	X	✓	✓ (19 July 2016)
	15 Nov 2016[a]	X	X	✓	✓
	28 Mar 2017[a]	X	X	✓	✓ (26 Mar 2017)

[a] Historical RPM data obtained from farmer, see also Section 2.5.

2.3. Sentinel-2A image post-processing

The workflow for image post-processing was developed to prepare the S2A imagery for the retrieval. The Sentinelsat library enables the automation of searching and downloading of satellite images from the Copernicus Open Access Hub (https://scihub.copernicus.eu/) using a cloud contamination threshold. Selected images were then processed with the Sen2Cor processor [version 2.3.0; European Space Agency. http://step.esa.int/main/third-partyplugins-2/sen2cor/ (accessed June 2017)], which performs topographic correction and transforms top-of-atmosphere reflectance to bottom-of-atmosphere reflectance. Scene classification and cloud masks are produced for each scene in the Sen2Cor process to allow for cloud and shadow removal, if required, prior to further analysis.

2.4. LAI retrieval algorithm

2.4.1. PROSAIL inversion approach

In our analyses, we consider two datasets (Fig. 2a) for testing *LAI* retrieval – ground hyperspectral data and actual S2A multispectral images. The ground hyperspectral reflectance data were resampled into the S2A bands using spectral response functions obtained from the European Space Agency's website (http://www.esa.int/ESA). These resampled data will be referred as '*in-situ* S2A' data hereafter. We were mainly interested in working with spectral bands (490, 560, 665 & 842 nm) corresponding to 10 m spatial resolution S2A images as some of our paddocks are relatively small in size; however, the retrieval scheme was also tested using resampled bands corresponding to the S2A 20 m bands (705, 740, 783, 865, 1610, 2190 nm).

The PROSAIL model was used to generate a Look-Up Table (LUT) of spectral reflectance for inversion. PROSAIL is a canopy radiative transfer scheme that couples leaf (PROSPECT) and canopy (4-SAIL) radiative transfer models (Jacquemoud et al., 2009; Jacquemoud and Baret, 1990; Verhoef, 1984; Verhoef and Bach, 2007). The model requires the following parameters: *LAI*, leaf inclination angle, hotspot parameter (q), leaf chlorophyll content (C_{ab}), leaf dry matter content (C_m), leaf water content (C_w), leaf brown pigment content (C_{bp}), leaf structure parameter (N), and the solar and viewing geometry (see also Table S1 in Supplementary material). Canopy level reflectance has been found to have a relatively small sensitivity to N (Punalekar et al., 2016) and S2A rarely samples in the sensitive hotspot zone; thus reflectance is

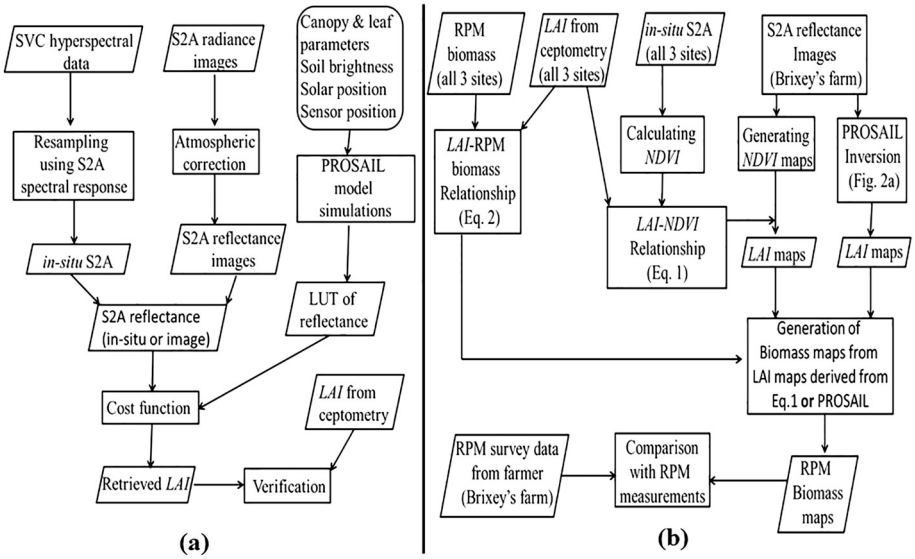

Fig. 2. Flowcharts showing (a) PROSAIL inversion scheme for *LAI* retrieval, (b) *LAI*-RPM biomass relationship generation and application over Brixey's farm to create S2A-based RPM biomass maps.

only modestly affected by *q*, in the nadir viewing direction (or even up to 5°, as in S2A scenes). Hence these parameters were fixed to 1.6 and 0.05 (both unitless), respectively.

The effect of leaf inclination is taken into account by using a leaf inclination distribution function (*LIDF*) that requires two parameters: $LIDF_a$ and $LIDF_b$ (both unitless). The first one defines the type of leaf inclination (with values between approximately −1, for fully erectophile, to +1 for planophile distributions) while $LIDF_b$ represents the bimodality of the distribution (Verhoef, 1998). Canopy reflectance is typically not strongly affected by $LIDF_b$; hence this parameter was fixed to −0.15, *i.e.* the default value of the standard PROSAIL model configuration.

The LUT was generated for six free parameters – *LAI*, C_{ab}, C_m, C_w, C_{bp} and $LIDF_a$. Twenty thousand random combinations of these parameters were generated within pre-defined parameter ranges. *LAI*, C_{ab}, C_m and C_w were sampled using a distribution function suggested by Weiss et al. (2000). $LIDF_a$ and C_{bp} were sampled assuming uniform distributions. Parameter values were allowed to range considerably in order to reflect the variability in herb and grass species at some of the sites (see Table S1). Parameter ranges were based on the literature, field data and previous research conducted on semi-natural grasslands (Darvishzadeh et al., 2008; Vohland and Jarmer, 2008; Atzberger et al., 2015; Punalekar et al., 2016). LUTs were generated for different solar and sensor zenith angles with respect to different observation dates and time (for S2A images as well as *in-situ* S2A).

The effect of soil type and soil moisture status on reflectance was also taken into account in the PROSAIL simulations by incorporating a semi-empirical soil reflectance model (Verhoef et al., 2018). This model simulates soil reflectance as a function of soil moisture content and three other soil parameters: soil brightness, soil 'latitude' and soil 'longitude'. Prior to performing PROSAIL simulations, we used *in situ* bare soil spectral measurements (for CEDAR farm and Sonning farm separately) to invert the soil model and obtain these soil parameter values for each soil type. As no bare soil measurements were available for Brixey's farm, retrieved values for CEDAR farm soil type were used. Soil moisture data (at 5 cm depth), obtained from a Vantage Pro2 weather station (Davis Instruments, USA) installed at CEDAR farm, were used to estimate soil moisture status on *in situ* sampling and S2A image acquisition days. In the model, two values of volumetric soil moisture content (0.2 and 0.4 $m^3 m^{-3}$) were considered, and LUT simulations were done for these two soil moisture scenarios and respective soil parameters derived for that site.

The contrast cost function (Verrelst et al., 2014) was used to find the best match between measured and modelled (from LUT) spectra. This function has been found to be more appropriate than the traditionally used cost functions (*e.g.* those based on root mean square error), particularly so for *LAI* retrievals (Rivera et al., 2013; Verrelst et al., 2014). In order to reduce effects caused by the ill-posed nature of inversion problems, parameters for the 50 best solutions (corresponding to the 50 lowest values of the contrast function) were averaged to calculate modelled estimates of all free parameters (Weiss et al., 2000).

2.4.2. NDVI based approach

In order to compare the radiative transfer model inversion to an empirical *NDVI* based approach in capturing changes in pasture biomass, *LAI* was also independently estimated from *NDVI*. The comparison was done for Brixey's farm and in terms of RPM derived biomass (Section 2.5).

All the *in-situ* S2A data (NIR: 842 nm and Red: 665 nm) and field measured *LAI* over CEDAR and Sonning farm were utilized to develop the following *NDVI-LAI* relationship (see also Fan et al., 2009; Gowda et al., 2016, for similar equations):

$$LAI = 0.001\exp^{(8.7343NDVI)} \quad (1)$$

This relationship was then applied to *NDVI* maps for Brixey's farm (derived from S2A) to generate a *LAI* map (for a summary of the procedure, see Fig. 2b). There were twelve S2A scenes for this farm from 19 July 2016 to 14 June 2017.

2.5. Generation of RPM biomass map from LAI and comparison with historical plate meter biomass data for Brixey's farm

S2A Image based *LAI* verification was not possible for Brixey's farm, due to lack of *LAI* measurements. However, historical RPM based indirect biomass measurements (Table 1), collected by the farmer, for Brixey's farm offered an opportunity to assess the usefulness of S2A images, combined with different retrieval procedures (PROSAIL and *NDVI* based, see Fig. 2), in capturing spatio-temporal variability in productivity on operational pasture farms. RPM derived biomass measurements were collected fortnightly as part of standard management practice and not for satellite verification specifically. Each record for a paddock on any given date corresponded to 30 random RPM measurements taken within that paddock. Dates of RPM collections were compared with the S2A image archive and three dates (19 July 2016,

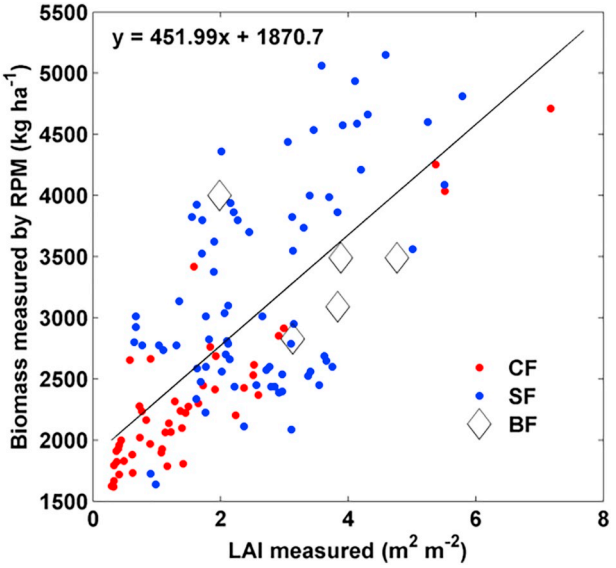

Fig. 3. Relationship between *LAI* and RPM biomass measurements (as reported in Eq. (2)) for all three experimental sites (CF, SF, BF representing CEDAR, Sonning and Brixey's farm respectively). Each symbol represents the average for one plot at any one date between March and August 2017 (Table 1). Note that Brixey's farm (4 plots) was sampled by the research team on 10 August 2017 only.

15 November 2016 and 26 March 2017) were identified for which good quality images were available within two days of the farmer's survey (Table 1).

The *LAI* maps (obtained by PROSAIL inversion as well as from the *LAI-NDVI* relationship (Eq. (1))) were converted into RPM based biomass values using a linear relationship (Eq. (2)) between field measurements for *LAI* and RPM readings. For this purpose, ground based *LAI* from ceptometry, and RPM measurements, as obtained by the research-team (procedures described in Section 2.2), for all three sites were pooled. A positive relationship was found between *LAI* and RPM measurements, BM (Fig. 3, $r^2 = 0.50$ and p-value for regression < 0.005), as defined by the following linear equation:

$$BM = 451.99 \times LAI + 1870.7 \quad (2)$$

Fig. 3 shows that generally lower values of *LAI* and biomass were found at CEDAR farm, whereas higher values were observed for Sonning farm (also reported in Figs. 4 and 5, for *LAI*). This was to be expected, as the small plots at Sonning farm were cut only occasionally and never grazed.

After creating biomass maps for Brixey's farm using *LAI* maps (Sections 2.4.1 and 2.4.2) and Eq. (2), paddock level averages were calculated using ARCMAP 10.4 spatial analyst toolbox (http://www.esri.com) and these were compared with RPM measurements, obtained by the farmer.

2.6. Verification procedures and statistics

In the case of the *in-situ* S2A bands derived from SVC data, *LAI* values retrieved for each individually measured spectrum were averaged to obtain the mean retrieved *LAI* per plot. For the S2A image verification (for CEDAR farm), retrieved *LAI* values of 4–5 pixels that fell well within each 30 m × 30 m sampling plot were averaged. The retrieved *LAI* average was compared with plot average *LAI*. The following statistics (using Matlab, Mathworks) were calculated in the context of *LAI* verification: Root mean square error (RMSE), r^2, slope of linear regression, range of modelled *LAI*, and concordance correlation coefficient (*crc*). The *crc* allows comparison of model simulations with measured values while correcting biases and considering them as independent variables.

3. Results

3.1. Comparison of measured and retrieved LAI: CEDAR farm and Brixey's farm

3.1.1. Changes in measured LAI with respect to weather conditions and management

Fig. 4a shows *LAI* measured with the ceptometer in three paddocks at CEDAR farm on different dates during spring and summer months in 2017. The silage plots (plots C9 and C10) had considerably higher *LAI* values than the grazed plots (C1–C8). The silage plots had been left ungrazed since the start of the growing season (approximately the first week of March) and had already reached *LAI* values of $> 5\,m^2\,m^{-2}$ by 11 April 2017. Further growth until 5 May 2017 increased *LAI* by a further 20%.

Weather conditions were conducive to good vegetation growth during spring (March–April). A steady rise in air temperature and incoming solar radiation since late winter (monthly average for February 2017: 6.5 °C, $3.80\,MJ\,m^{-2}\,day^{-1}$) through early spring (March 2017: 9.4 °C, $8.54\,MJ\,m^{-2}\,day^{-1}$, April 2017: 8.9 °C, $14.4\,MJ\,m^{-2}\,day^{-1}$) boosted pasture growth. The variations in *LAI* on the grazed plots during April–May were driven by vegetation growth as well as pasture removal due to grazing, and maximum *LAI* was always $< 4\,m^2\,m^{-2}$. Relatively low *LAI* values were found on 5 May 2017 and 25 May 2017, as the paddock had been grazed about 7–10 days before these dates. Very low *LAI* values were observed for 21 June 2017, resulting from drought-induced pasture die-back due to low rainfall and relatively high air temperatures (total rainfall between 10 and 25 June 2017 was 0.6 mm and average air temperature was 18.9 °C).

In general, considering the size of the individual error bars in Fig. 4a, *LAI* did not differ significantly between dates for plots C1 to C5, except on 21 June 2017. However, these relatively large error bars illustrate considerable within-plot variability. Plots C6–C8 in Paddock 6 (Fig. 1) were sampled twice (11 April and 21 June 2017). As they were grazed almost a month before 21 June 2017, grass regrew well before the water stress conditions occurred and hence these plots had higher *LAI* compared to C1 to C5, which were more susceptible to soil water deficiencies as they were grazed from 1 to 11 June 2017.

3.1.2. LAI verification with respect to ceptometry measurements

Fig. 4b and Table 2 (top row) show a comparison between measured *LAI* and *LAI* retrieved using PROSAIL (see Section 2.4.1, Fig. 2a) using *in-situ* S2A (10 m bands) simulated from SVC hyperspectral data.

Note that there were some small discrepancies between dates of *LAI* sampling, SVC survey and actual image acquisition; for example, on 5 April 2017 no SVC survey was done on plots C1–C5, but *LAI* measurements and a good quality S2A image (2 April 2017) were available.

High to very high values of *crc* and r^2 in Table 2 indicate that there was a good match between measured and modelled *LAI* for CEDAR farm and Brixey's farm (10 August 2017, 4 plots), when data for all SVC sampling dates were considered. Fig. 4b shows that high values of *LAI* for CEDAR farm silage plots (C9 and C10) on 11 April 2017, as well as highly reduced *LAI* values on 21 June 2017 for plots C1 to C5, were captured well by the PROSAIL inversion.

Fig. 4b also shows results for four herbal-grass mixture plots (B1–B4) that were sampled on 10 August 2017 at Brixey's Farm. Three out of four of these points fell close to the 1:1 line shown in the scatter plot; however, retrieved *LAI* for the grass plot with the highest measured *LAI* values (paddock no. 25) was lower than measured *LAI*. During August, paddocks at Brixey's farm were on a ~35 days rotation cycle and had favourable weather conditions (average air temperature 16.6 °C, rainfall 72.4 mm). Paddock number 25 (Fig. 1), that contained our sampling plots, was grazed on 12 July2017 and had achieved a

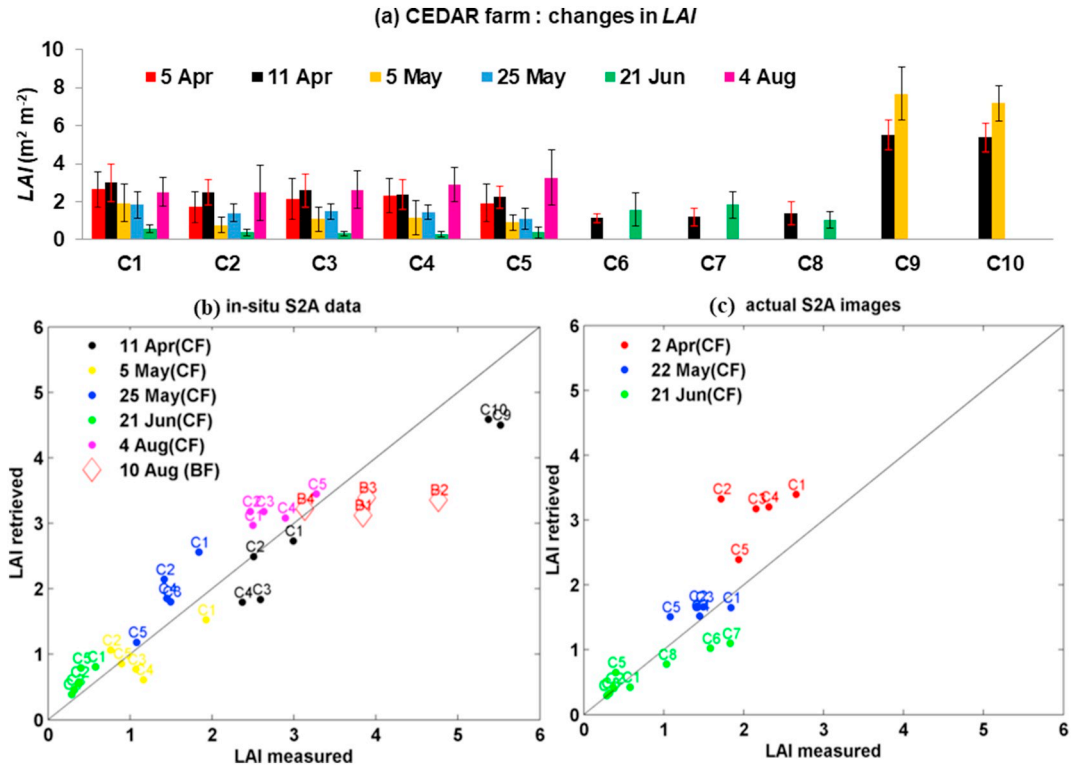

Fig. 4. (a) Variations in ceptometer measured *LAI* for sampling plots at CEDAR farm on different dates; (b) comparison between measured *LAI* and *LAI* retrieved from *in-situ* S2A bands at CEDAR farm (CF) and Brixey's farm (BF); (c) comparison between measured *LAI* and *LAI* retrieved from actual S2A images for sampling plots at CEDAR farm. All dates correspond to the year 2017.

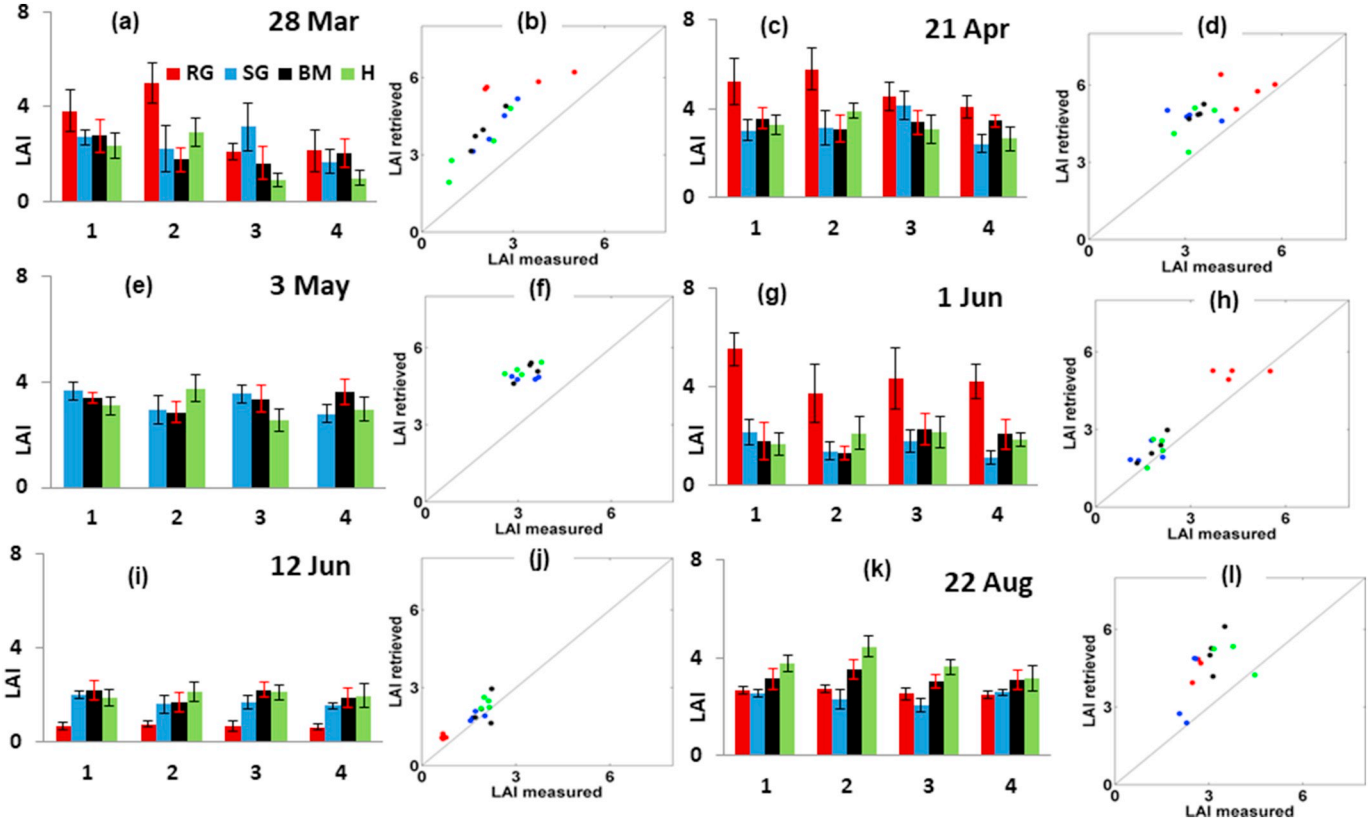

Fig. 5. (a, c, e, g, i, k) Bar charts showing variation in *LAI* among four pasture types (RG: ryegrass, SG: smartgrass, BM: biomix, H: herbal) over different sampling dates at Sonning farm. Each type had four replicates, as indicated by the error bars; (b, d, f, h, j, l) corresponding scatter plots show comparisons between measured *LAI* (ceptometry) and *LAI* retrieved from *in-situ* S2A for sampling plots at Sonning farm. All dates in the figure correspond to the year 2017.

Table 2
Statistics reporting a comparison between measured and retrieved *LAI* for all three sites.

Data	Spatial resolution corresponding to bands used (m)	Farms	RMSE ($m^2 m^{-2}$)	r^2	*slope*	*crc*	Range ($m^2 m^{-2}$)
In-situ S2A	10	CEDAR farm, Brixey's farm	0.55	0.87	0.78	0.88	4.20
In-situ S2A	10	Sonning farm	1.22	0.61	0.84	0.61	4.30
Actual S2A images	10	CEDAR farm	0.62	0.76	1.30	0.64	3.10
In-situ S2A	10 & 20	CEDAR farm, Brixey's farm	0.91	0.78	0.91	0.86	4.24
In-situ S2A	10 & 20	Sonning farm	1.19	0.56	0.73	0.58	3.96

dense vegetation cover by 10 August 2017 (average measured *LAI*: 4 $m^2 m^{-2}$).

Except for the aforementioned four plots from Brixey's farm and two CEDAR farm silage plots, all other points in the scatter plot (Fig. 4b) represent CEDAR farm sampling plots C1 to C5. For these plots the variations over different dates observed in measured *LAI* were also evident in the *LAI* retrieved from *in-situ* S2A. For example, both average measured and retrieved *LAI* on 11 April and 4 August 2017 were higher than average *LAI* on 5 May, 25 May and 21 June 2017 (Fig. 4a). However, retrieved *LAI* values for 11 April and 25 May 2017 were very similar, whereas the measured values show a much clearer separation between these dates.

Finally, Fig. 4c shows the comparison between measured *LAI* and *LAI* retrieved from *actual* S2A images (10 m bands), for CEDAR farm, for three different dates (2 April, 22 May and 21 June 2017). *LAI* measurements for plots C1–C5 conducted on 5 April and 25 May 2017 were used for comparison with *LAI* maps for 2 April and 22 May 2017, respectively. Three plots (C6–C8, sampled on 21 June 2017) were included in addition to the regularly measured plots C1–C5, dictated by availability of field *LAI* data (*in-situ* S2A data were not available for these plots; hence, they were not shown in Fig. 4b). Table 2 (third row) shows lower *crc* and r^2 values for retrievals based on *actual* S2A images compared to *in-situ* S2A retrieval. However, reasonable values of all statistical measures confirm good overall accuracy of the PROSAIL LUT retrieval algorithm using both datasets. Similar to observed *LAI*, retrieved values show high *LAI* on 5 April 2017 followed by 25 May 2017 and lowest values on 21 June 2017. However, the range of modelled *LAI* based on actual S2A data (3.1 $m^2 m^{-2}$) was relatively narrow compared to the observations (5.2 $m^2 m^{-2}$, based on all dates and sites combined) and *in-situ* S2A retrievals (4.2 $m^2 m^{-2}$).

Table 2 also shows statistics for *LAI* retrieval using *in-situ* S2A bands that correspond to 20 m as well as 10 m bands. With these additional bands included, there was a small drop in *crc* for CEDAR and Brixey's farm (compared to row 1 in Table 2); however, *RMSE* and r^2 were significantly poorer compared to the retrieval using the 10 m bands only.

3.2. Comparison of measured and retrieved LAI: Sonning farm

3.2.1. Changes in measured LAI with respect to weather conditions and management

Fig. 5 shows bar plots summarising ceptometry-based *LAI* measurements for four pasture types (four replicates of each type, see Section 2.1) for small plots at Sonning farm, as observed on different sampling dates. The seasonal growth pattern of the forage species monitored here varies, with most legumes, chicory and plantain being dormant or semi-dormant at cooler temperatures in the winter, whereas growth peaked in late spring and summer.

Ryegrass grows at cooler temperatures and has higher growth rates in early spring and autumn compared to other grasses and herbal mixtures (Kemp et al., 2010). Hence, on most sampling dates, it was found to have significantly higher *LAI* values than the other pasture types. Due to their rapid growth, plots with ryegrass were cut earlier than other pasture types. Hence there were no measurements of *LAI* on 3 May 2017 as ryegrass plots was cut a week before this date and the grass crop was still too low to reliably conduct ceptometry. Similarly, on 12 June 2017 *LAI* for ryegrass was less than the values measured for the other types, due to the fact that ryegrass was cut on 1 June 2017 and left to re-grow, while the other pasture types were left uncut to achieve maximum biomass stage. The rapid growth of ryegrass was reduced in late summer, when herbal plots started to grow more vigorously and hence had higher *LAI* on 22 August 2017, compared to ryegrass. Other than on 22 August 2017, measured *LAI* was not significantly different among biomix, smartgrass and herbal plots.

Weather conditions at Sonning farm were very similar to CEDAR farm due to their geographical proximity. However, Sonning farm plots generally had higher *LAI* values compared to CEDAR farm due to the absence of grazing. These plots were comparable to the silage plots at CEDAR farm.

3.2.2. LAI verification with respect to ceptometry measurements

Each bar chart in Fig. 5 is paired with a scatter plot that shows a comparison of measured *LAI* against *LAI* retrieved using four *in-situ* S2A bands. Plots corresponding to dates with ryegrass (all except 3 May 2017), having the highest measured *LAI*, also showed the highest retrieved values (28 March, 21 April and 1 June 2017). Retrieved *LAI* was lowest for ryegrass on 12 June 2017, as was also observed in the measurements. Furthermore, on 22 August 2017 retrieved *LAI* values for ryegrass were comparable to those obtained for other forage species. Also, those retrieved for herbal plots were considerably higher than values for most of the non-ryegrass plots. Likewise, these findings correspond well with the observed variations in *LAI* on 22 August 2017. In general, retrieved *LAI* was overestimated for all dates and especially for plots with observed *LAI* $> 3 m^2 m^{-2}$.

The statistical indicators relating to Sonning farm (second row of Table 2) indicate a reasonably good accuracy of *LAI* retrieval. Similar to the other two sites, inclusion of 20 m bands (*in-situ* S2A only) did not improve retrieval accuracy any further.

3.3. Spatial maps of LAI: CEDAR farm

Fig. 6 shows S2A-derived *LAI* maps for CEDAR farm for three dates – 5 April, 22 May and 21 June 2017. Verification of retrieved *LAI* has been reported for these dates in Section 3.1.2. These maps show spatio-temporal changes in *LAI* for all paddocks, which were in parity with expected changes in pasture vegetation, as driven by weather conditions and management operations. High *LAI* in most of the paddocks on 2 April 2017 can be explained by good growth of perennial ryegrass pastures in early spring (from early March onwards). The weather during March was relatively warm and sunny (compared to the long-term average) and the soil moisture content was near field capacity. Most of the paddocks did not have cows grazing until 2 April 2017. Grazing commenced on all paddocks and more or less followed a rotational pattern, during April and May. Some paddocks were also cut for silage, which resulted in pronounced differences in *LAI* among paddocks on 22 May 2017.

Later in the growing season, around 21 June 2017, all paddocks had a distinctly low *LAI* due to plant water stress (as discussed in Section 3.1.1). Ryegrass generally has a low tolerance to soil moisture deficits (Akmal and Janssens, 2004) due to its relatively shallow root zone and

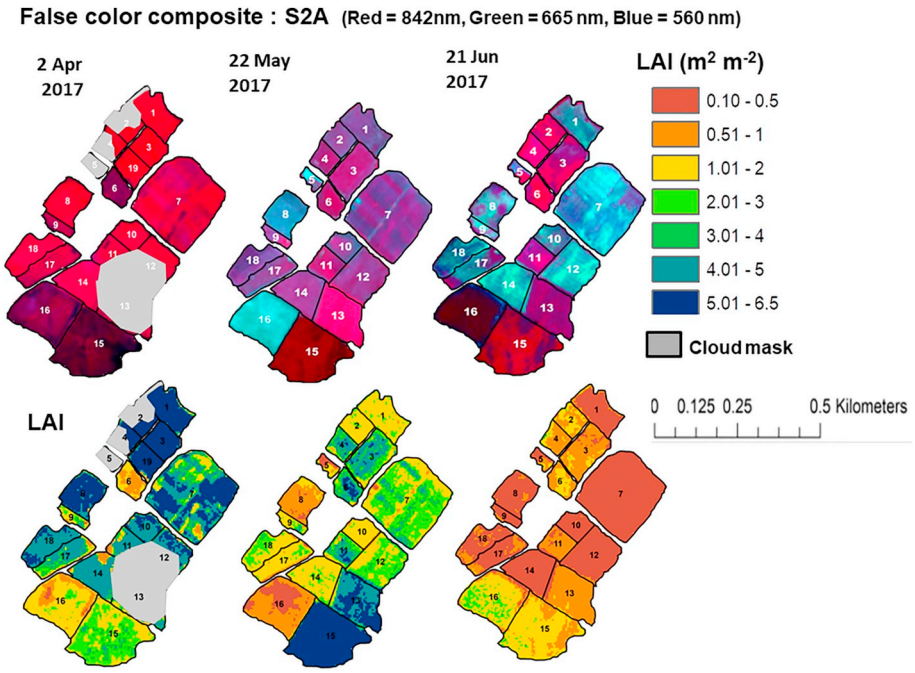

Fig. 6. False colour composite S2A images (top row) of CEDAR farm for three dates in 2017 used for determination of *LAI* maps (bottom row) using the PROSAIL model inversion.

hence most paddocks in CEDAR farm experienced drought, resulting in grass die-back for the period around 21 June 2017. This can be clearly seen in the *LAI* map produced for that date.

Paddock 8 was under silage around 2 April 2017 and hence had $LAI > 5\,m^2\,m^{-2}$, whereas its *LAI* was $< 1\,m^2\,m^{-2}$ on 22 May 2017, as the sward was cut in the middle of May.

Note that some distinct strips are visible in paddock 7; it had a variety of pasture mixtures grown in strips (Sections 2.1 and 2.2); these are most distinct on 22 May 2017. However, on 21 June 2017 the entire paddock had $LAI < 0.5\,m^2\,m^{-2}$ as it was cut for silage on 12 June 2017.

3.4. Spatial maps of biomass based on PROSAIL and NDVI retrieval: Brixey's farm

Fig. 7 shows RPM-equivalent biomass maps for Brixey's farm, produced from PROSAIL derived *LAI* maps (Fig. 2a) and Eq. (2). These maps showed considerable spatio-temporal variability for the different grazing paddocks.

Changes in pasture cover brought about by grazing/cutting for silage can be easily traced in the maps, especially for images captured by consecutive S2A passes (~12-day periods; see, for example, maps for 3 and 15 November 2016 or 13 and 26 March 2017). In these cases, abrupt drops in biomass were caused either by grazing or removal of pasture for silage. Paddocks with biomass lower than $\sim 2000\,kg\,ha^{-1}$ indicated freshly grazed or cut paddocks; in subsequent biomass maps they exhibited increased biomass, showing that they had been left to recover.

Statistics relating RPM-equivalent biomass maps derived from PROSAIL (Eq. (2) and Fig. 2b) with actual surveys for three dates (Table 1) have been reported in Table 3 (left side). Values for r^2 and RMSE indicate relatively poor agreement between modelled and measured biomass when all three dates were compared together. However, when the comparison was done separately for each date, RMSE and *crc* values improved for all dates. Values of *crc of* 0.50 or higher, and $r^2 > 0.40$, on all three dates indicated a reasonable match between modelled and measured RPM biomass estimates (p-value for regression < 0.005). However, values were clearly overestimated (high RMSE), especially on 15 November 2016 and 26 March 2017 (Fig. 8a).

Fig. 8b and Table 3 (right side) also report on the agreement between *NDVI* based biomass maps and RPM surveys. Higher r^2 and lower intercept (in magnitude) indicate a better linear fit between measured and modelled RPM biomass estimates using PROSAIL based *LAI* maps than when *NDVI* based once. RMSE was also lower for PROSAIL inversion based biomass maps for 'all three dates' and 19 July 2016 maps. However, *NDVI* based biomass estimates were slightly more accurate in terms of *crc* and RMSE for 15 November and 26 March data. It is important to note that the standard deviation bars plotted for modelled average biomass depict within-image spatial variability and these bars were longer for inversion based biomass maps compared to *NDVI* based ones. This is also demonstrated by the higher range in biomass, for inversion based maps (Table 3, left side).

Note that all the pixels within a given paddock boundary were used to calculate average RPM based biomass estimates (Figs. 7 and 8). Pixels close to the paddock boundary may have been affected by the area surrounding the paddock (Handcock et al., 2008) and this may help explain the relatively poor fit between observations and S2A estimates. However, these errors should have had a similar effect on both PROSAIL based and *NDVI* based *LAI* maps. Therefore, we did not omit any edge pixels when comparing these two methods for *LAI* retrieval (and hence for generation of RPM biomass maps).

4. Discussion

4.1. Performance of the retrieval scheme using S2A data

Since the Sentinel optical satellites mission was proposed, various studies have examined the potential of Sentinel 2 bands, resampled from field/airborne hyperspectral sensors, for the monitoring of a wide range of crops including pastures (Delegido et al., 2013, 2011; Frampton et al., 2013; Sibanda et al., 2015). The findings presented in our paper that use *in-situ* S2A bands resampled from SVC hyperspectral data are consistent with those studies and demonstrate the potential of using Sentinel 2 data for observing grass vegetation dynamics.

The good accuracy of the PROSAIL based *LAI* retrieval algorithm, using *in-situ* S2A data, for typical perennial ryegrass (CEDAR farm) as

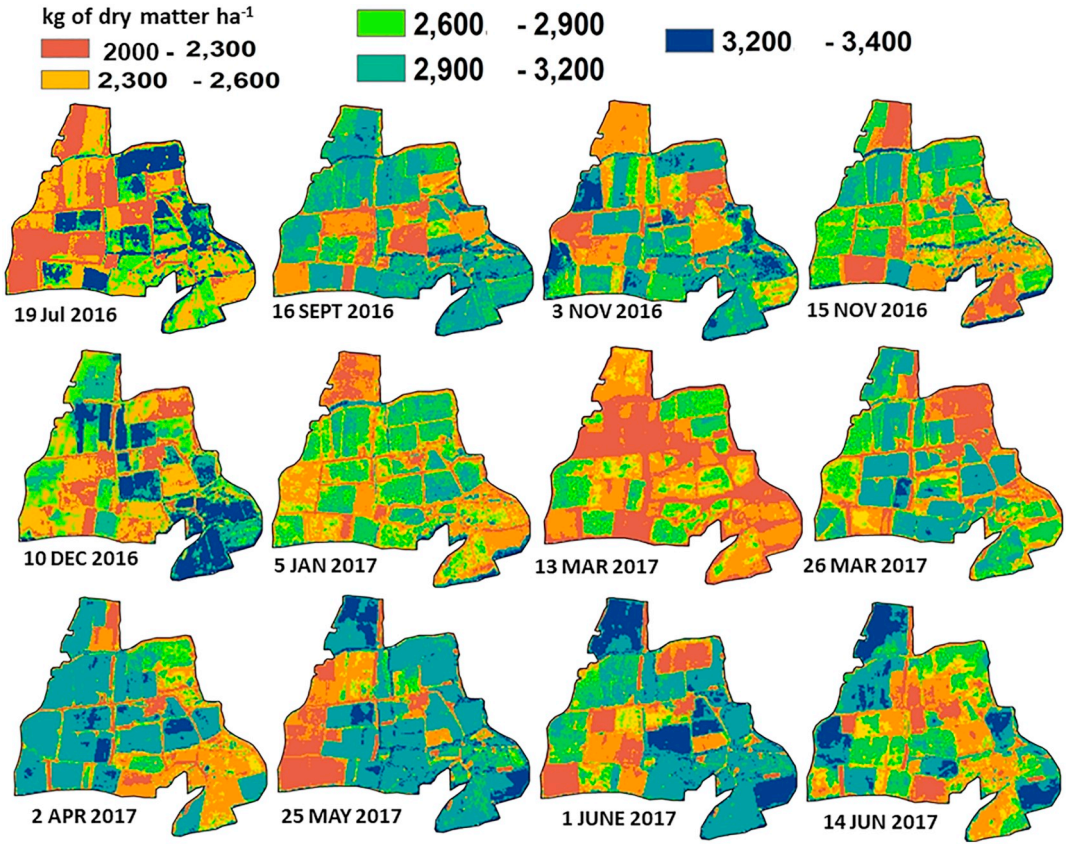

Fig. 7. S2A based RPM-equivalent biomass maps for Brixey's farm corresponding to dates in 2016–17, produced by applying Eq. (2) on twelve *LAI* maps (not shown) derived from S2A images through PROSAIL inversion.

well as herbal-legume-grass mixtures (Sonning and Brixey's farm) has shown that S2A bands with 10 m spatial resolution can be used to monitor growth of pastures with variable composition and for different farm management configurations (grazed *versus* un-grazed, as well as silage plots). This is important from a sustainable management point of view, as this practice encourages a good balance between the use of traditional perennial ryegrass and herbal pastures for optimising both pasture quality and quantity for dairy and meat production (Sleugh et al., 2000; Woodward et al., 2013).

Furthermore, this study is among the very few, if not the first, research work that reports image based verification of pasture biophysical properties derived from S2A. Our results show (Table 2) that actual image based retrievals over perennial ryegrass (CEDAR farm) were better than *in-situ* spectral data based retrievals for pasture mixtures at Sonning farm. This is related to a better performance of the retrieval algorithm over 'relatively homogeneous' and less dense ($LAI < \sim 4\ m^2\ m^{-2}$) canopies in regularly grazed perennial ryegrass paddocks. The good performance of PROSAIL S2A image based retrievals during three different stages of canopy growth at CEDAR farm (Figs. 4c and 6), indicates that the post-processing techniques and corrections (geometric, radiometric and atmospheric) were reliable, and that the field based sampling strategies for verification were appropriate. Furthermore RPM-equivalent biomass maps derived using *LAI* maps (Eq. (2), Fig. 2b) created for Brixey's farm, using PROSAIL inversion (Fig. 2a), captured within-paddock spatial variability well.

Our study *overestimated LAI* values for Sonning farm plots that had relatively high *LAI* (Fig. 5). The increased discrepancy between modelled and measured *LAI* for Sonning farm, in comparison to CEDAR farm, may partly be explained by the fact that the Sonning plots were characterised by multi-species 'swards' with a broader range and larger number of possible combinations of biophysical and chemical properties at leaf and canopy scale. These kinds of canopies pose a challenge to radiative transfer models such as PROSAIL that assume canopies to be a homogeneous medium. Although PROSAIL based inversions have been proven to be sufficiently accurate for a wide range of canopies, including heterogeneous grasslands, reductions in accuracy of

Table 3
Brixey's farm biomass analyses: statistics summarising a comparison between farmer-collected RPM biomass measurements and RPM biomass calculated using *LAI* maps derived from a combination of PROSAIL inversion and Eq. (2) (see also Fig. 8a); or based on a *NDVI* based empirical equation for *LAI* (Eq. (1)) and Eq. (2) (see also Fig. 8b).

	RPM measurements compared with RPM-equivalent biomass estimates using *LAI* maps from PROSAIL inversion and Eq. (2)				RPM measurements compared with RPM-equivalent biomass estimates using *LAI* maps from *NDVI* and Eq. (2)			
Statistics	All three dates	19-Jul-16	15-Nov-16	26-Mar-17	All three dates	19-Jul-16	15-Nov-16	26-Mar-17
RMSE (kg ha^{-1})	802.93	488.50	881.73	990.37	717.60	524.97	830.60	784.94
r^2	0.22	0.46	0.54	0.76	0.16	0.38	0.40	0.73
slope	0.55	0.52	1.14	1.42	0.41	0.44	0.71	1.20
Range (kg ha^{-1})	2030.93	1697.40	1537.01	1877.10	1869.68	1433.30	1404.99	1738.08
crc	0.45	0.59	0.53	0.57	0.40	0.50	0.62	0.69

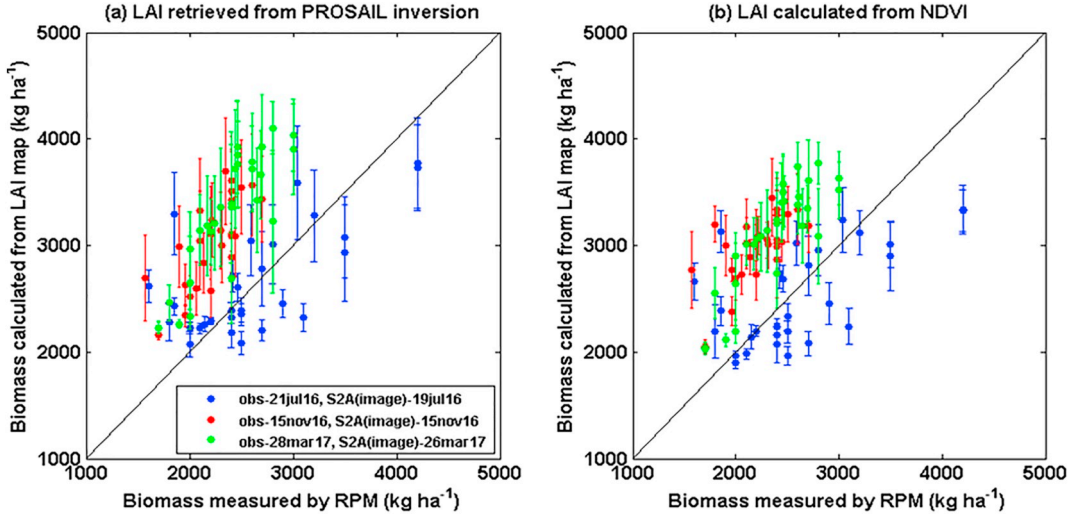

Fig. 8. (a) Comparison between farmer RPM biomass measurements and RPM biomass equivalent maps derived from *LAI* maps obtained *via* PROSAIL inversion and using Eq. (2). (b) As described in (a), but in this case *LAI* was derived from *NDVI* using Eq. (1). Both measured and calculated biomass values were averaged at paddock level. Each dot represents one paddock on Brixey's farm, with the spatial variability (based on a variable number of pixels per paddock) indicated by the error bars.

algorithms with increased species diversity in grasslands have also been reported in the literature (Darvishzadeh et al., 2008).

The performance of *LAI* retrieval schemes has also been linked to the sensitivities of reflectance to *LAI* in different spectral regions (VIS, red-edge, NIR and SWIR). Reflectance in the NIR is highly sensitive to *LAI*. However, opinions differ regarding the importance of red-edge bands, as this region of the spectrum corresponds to a shift from chlorophyll absorption to leaf scattering (Darvishzadeh et al., 2009; Delegido et al., 2011; Herrmann et al., 2011; Richter et al., 2012). In our study inclusion of red-edge bands, obtained from the 20 m resolution S2A data, did not lead to an improvement in *LAI* retrieval. Nevertheless, the retrieved *LAI* using either bands corresponding to 10 m, or to 10 and 20 m combined, compared reasonably well with measured *LAI* as illustrated by high and comparable *crc* values (Table 2). This implies that the exclusion of red-edge bands, while producing 10 m *LAI* maps using just four S2A bands, would probably not affect retrieval accuracy for pasture canopies. However, red-edge bands have been found to be useful for retrieval of other crucial parameters such as chlorophyll content (Clevers and Gitelson, 2013) and hence this additional information has the potential to further aid pasture management activities such as fertilizer applications and therefore needs further investigation.

The inclusion of the 20 m band centred on 1610 and 2190 nm also did not improve *LAI* retrieval accuracy (Table 2), despite the fact that SWIR bands have been reported to be beneficial for *LAI* or biomass retrieval by some researchers (Darvishzadeh et al., 2009; Richter et al., 2012). For example, Handcock et al. (2008) recommended utilization of SWIR bands in biomass estimation to characterize seasonal as well as management driven changes in non-photosynthetic material, together with the contribution of soil fractions, on the canopy reflectance. Effective utilization of SWIR bands in improving *LAI* retrieval through LUT inversion may be achieved by improved representation of leaf dry matter and water content in the LUT parameters, as well as modification of the background soil spectra for litter content (Danner, 2017). This may require characterization of seasonal and management driven changes in senescing plant material that affect SWIR bands reflectance, which in turn would provide an additional source of information aiding *LAI* retrieval.

4.2. Comparison between PROSAIL derived and NDVI based biomass maps

Our analyses showed that LUT based biomass predictions (using Eq. (2) and the approach outlined in Fig. 2b to get biomass from *LAI*) performed better than *NDVI* based biomass maps. Although model comparison statistics were not largely different for *NDVI* based and LUT based retrievals (Table 3), it is important to note that LUT based inversions for *LAI* were *independent* of field based information; whereas the *NDVI* based *LAI*-equation was developed using field measurements. In addition, standard deviation bars in Fig. 8 show that LUT based biomass maps exhibited more within-paddock variability compared to *NDVI* based biomass maps. Thus, non-dependence on field based information, and improved accuracy, demonstrate that LUT based *LAI* retrieval schemes offer better and more versatile options for operational systems dedicated to regular pasture monitoring. Note that remote sensing indices that include further S2 bands, in addition to those used for *NDVI*, may be more successful in determining biomass for pasture land (Delegido et al., 2011; Handcock et al., 2008). However, spectral statistical models would always need larger calibration datasets than a physically based model, before they can be used for operational systems.

The moderate accuracy of the *LAI*-RPM relationship in addition to its empirical nature suggests that Eq. (2) is not readily transferable for pasture monitoring over different sites in operational systems. The weakness of the relationship is potentially a result of the indirect nature of both RPM and *LAI* measurements. Furthermore, the lower r^2 and *crc* when comparing remotely sensed biomass (obtained *via* remotely-sensed *LAI* and Eq. (2), which is based on a combination of RPM measurements and *LAI* derived from ceptometry) and actual RPM observations (Fig. 8 and Table 3) could also be due to the fact that the farmer only took 30 measurements (compared to the recommended 50–80) per paddock to derive paddock average biomass. The comparison is particularly poor when all dates have been combined (Table 3), which indicates that the nature of the relationship between *LAI* and RPM, as well as RPM calibration equations, are dependent on season. In fact, seasonal changes in RPM calibrations have been discussed in the literature (Thomson et al., 1997). However, recommendations from such papers are generally not implemented by commercial instrument manufacturers, as the country or region where the RPM will be used is not known. The responsibility to correctly 'set up' the RPM lies with the user and the requirement to adopt the appropriate conversion equation, and the implication of inaccurate biomass predictions, are not communicated well to farmers.

Despite the only moderate goodness of fit of the *LAI*-RPM relationship, we used it to generate remote sensing based RPM-equivalent

biomass maps, not so much to promote it as a model for pasture biomass estimation, but rather to allow us to study and comment on within-paddock variability, as well as provide the opportunity for a comparison between PROSAIL based and *NDVI* based retrieval methods.

4.3. Sentinel 2 based operational system for pasture monitoring

The LUT algorithm we have presented here is designed as a proof-of-concept for how such a retrieval might be implemented with Sentinel-2 data. It is not, in its current form, likely to be useful as an operational tool but could serve as a starting point to develop one. LUTs are used already for some operational satellite derived products, for example the MODIS LAI/fAPAR algorithm (Myneni et al., 1999) and there are a number of techniques that could be used to speed up the inversion of our algorithm. For example Gastellu-Etchegorry et al. (2003) present a method that generalises LUTs for view-illumination geometries which eliminates the need to produce individual LUTs for each scene as done in our study. Verrelst et al. (2014) suggest a method that involves the combination of multiple best solutions with the addition of noise. Here we have opted only to use the multiple best solution component, but the addition of noise is something that could potentially form part of an operational algorithm. Many other disciplines use LUTs routinely and there are inevitably valuable methods that could be incorporated in operational systems used for pasture monitoring. For example, Wilcox et al. (2011) describe a tool, Mesa, that provides a range of performance enhancements for LUTs that remove a large number of design decisions from the construction of the LUT. Verrelst et al. (2015) discuss various hybrid retrieval schemes essentially developed to speed up biophysical mapping in operational systems. We propose that further research can build on these research findings.

Apart from the technical aspects of the actual operational algorithm it is important to discuss essential features of operational systems from the user's perspective. Considering the dynamic nature of intensively managed grazing pastures, Eastwood et al. (2009) posed that for any pasture monitoring system to be efficient and reliable three factors play a key role – timeliness, efforts in data collection and accuracy. By definition remote sensing based solutions should reduce the manual efforts involved in pasture monitoring. Furthermore, with the advent of software and hardware tools that can handle large datasets in real time it is becoming easier to deliver final biomass prediction products in user friendly formats to farmers (pasture wedge plots for instance) within a couple of days of image acquisition. However, even though in theory the Sentinel 2 program offers an excellent spatial coverage approximately every 5 days (depending on latitude), in countries such as the UK frequent cloud cover significantly reduces the number of good quality satellite scenes. Based on the MODIS cloud mask analysis for the UK, Armitage et al. (2013) showed that mean percentage of cloud free days in the UK in 2005 was only 21.3%. Thus, delivering biomass maps whenever a good satellite image is available may not be a viable approach for efficient pasture management. Hence our future work will focus on combining retrieved *LAI* maps with a pasture growth model to produce full time-series of pasture biomass estimates, taking into account the management activities and weather conditions. These estimates will be verified using actual (destructive) biomass measurements. This may allow the delivery of biomass prediction maps in near-real time, thus assisting farmers in well-informed management decisions such as designing weekly grazing rotation plans.

The accuracy of biomass estimates has a significant effect on biomass allocation and feed supplements and hence on overall input cost and profit margin. The level of accuracy expected from a prediction tool has been found to be dependent on the individual famer's perception and management practices (Eastwood et al., 2009). At Sonning and CEDAR farms a prediction accuracy of about 100 kg DM ha^{-1} is considered to be the ideal target by the farm management. For example, with the accuracy of 100 kg DM ha^{-1} and estimated intake of 15 kg DM per dairy cow per day, stocking density could still be under or over estimated by ± 6.7 animals or 6.7%. Traditional methods such as RPM can provide an accuracy of about 350 to 450 kg DM ha^{-1} (Huillier and Thomson, 1988; Thomson et al., 1997) which at a target available biomass of 1500 kg DM ha^{-1} produces a biomass prediction error of up to 30%.

In absence of any destructive (and hence more accurate) biomass measurements it is difficult to discuss the absolute accuracy of the biomass maps derived from *LAI* maps in this paper. Table 3 shows a sub-optimal predictive performance of our derived RPM-*LAI* relationship resulting in an overall high RMSE for RPM-equivalent biomass maps (reasons for this are discussed in Sections 3.4 and 4.2). In order to approximate the potential error in biomass maps purely due to errors associated in the *LAI* maps, RMSE in retrieved *LAI* (Table 2) was translated to biomass units using a *LAI*-RPM derived biomass equation (Eq. (2)). The calculated error was about 250 kg ha^{-1} in the grazing paddocks and ~550 kg ha^{-1} in mixed pasture silage plots, which is considerably better and somewhat worse, respectively, than the error-range reported for plate-meters. Therefore, there is scope for improving the accuracy of biomass predictions based on remotely-sensed *LAI* maps. This can be achieved by expanding the LUT for a range of pasture types and seasonal variations in the pasture canopy, thereby taking into account the inherent variability in biophysical parameters and combined effects of soil and litter fractions on canopy reflectance, but most importantly by combining the potential of satellite images with that of process-driven pasture growth models. We propose to use the *LAI* maps (containing key spatial information in terms of pasture density distribution) as assimilation datasets for a pasture growth model. This model uses daily weather data to predict near-real time changes in pasture biomass, to inform management decisions. The pasture growth model simulates daily values of biomass and *LAI* and whenever a good-quality Sentinel 2 image is available a *LAI* map would be derived as per the procedure described in this paper. During the generation of pasture *LAI* maps a calibration routine minimises the difference between the remotely sensed *LAI* and growth model simulated *LAI* by calibrating photosynthesis and growth related parameters. The developed pasture monitoring system would ultimately use weather forecast data to generate biomass growth predictions and hence can be used to create so-called pasture wedge plots to help farmers develop grazing rotation plans across paddocks. Similar remote sensing based model assimilation algorithms have been proposed for arable crop monitoring (Dorigo et al., 2007; Olioso et al., 2005). However, in the case of intensively grazed pastures, for which remote sensing based applications are currently largely empirical, and pasture growth models are rarely used in conjunction with remote sensing based datasets, the proposed algorithm would explore new solutions to regular monitoring as well as more informed decision making. We emphasise that full advantage of fine spatiotemporal satellite datasets for pasture management demands further research in development of such model-data fusion tools.

5. Conclusions

We have demonstrated that Sentinel 2A data, combined with a radiative transfer model (PROSAIL), can be used for pasture monitoring at high spatio-temporal resolutions and with good accuracy. The 10 m spatial resolution allows for assessment of within-paddock variability due to selective grazing, for example, and can be used by farmers to identify farm management problems. The physically based approach outperforms the empirical NDVI approach, as it does not require site specific calibration of the retrieval model and in theory has the potential to be applied and tested over a wide range of farms without requiring a large field based database. Despite the fact that PROSAIL should theoretically work best with homogeneous canopies, we obtained good results for both homogeneous and mixed species forage plots and paddocks, which is encouraging for farmers moving away from single species herbage feeds. We postulate that Sentinel 2A-

derived field-average biomass estimates, as well as their spatial variability, are potentially better than those derived from rising plate meter surveys. However, to predict biomass yield, for example to help pasture farmers manage their feed wedge, the S2-PROSAIL package would need to be combined with a comprehensive process-based grass growth model, driven by weather predictions. In a follow-up paper, we will present such an approach, that allows for single-species and multi-species swards and that will work in conjunction with the inversion algorithm presented here, to provide day-by-day current and near-future estimates of grass productivity and other key sward parameters.

Acknowledgements

We would like to thank Innovate UK for funding the PASQUAL project (Monitoring and prediction of pasture quality and productivity from satellites; Innovate UK Project No: 102681). Tristan Quaife's contribution was part funded by the NERC National Centre for Earth Observation (NCEO). The Sonning and CEDAR Hall farm mixed forage plots have been designed and maintained as part of the BBSRC SARIC biodiverse forages project (Project BB/N004353/1). We thank our project partner organisation, Rezatec, for their support and collaboration. We are grateful to the Natural Environment Research Council (NERC) Field Spectroscopy Facility, based at Edinburgh University for providing us with the second SVC field hyperspectral instrument (loan reference 752.1116), and in particular to Chris MacLellan for his guidance on how to configure and use the dual-instrument set-up. We also thank Mr Clyde Jones for providing farm data for and access to Brixey's farm. In addition, we acknowledge the contributions of farm manager James Lamburn, who has been helpful regarding issues related to CEDAR Hall farm. Christiaan van der Tol and Wout Verhoef have given valuable advice with regards to the PROSAIL code and parameters, and issues relating to soil reflectance modeling. Finally, we thank those who helped us out in the field, Pierre-Antoine Ariotti, Kirsten Lees, and Anna Thomson in particular.

Appendix A. Supplementary material

Supplementary data to this article can be found online at https://doi.org/10.1016/j.rse.2018.09.028.

References

Akmal, M., Janssens, M.J.J., 2004. Productivity and light use efficiency of perennial ryegrass with contrasting water and nitrogen supplies. Field Crop Res. 88, 143–155. https://doi.org/10.1016/j.fcr.2003.12.004.

Ali, I., Cawkwell, F., Dwyer, E., Barrett, B., Green, S., 2016. Satellite remote sensing of grasslands: from observation to management. J. Plant Ecol. 9, 649–671. https://doi.org/10.1093/jpe/rtw005.

Armitage, R.P., Alberto Ramirez, F., Mark Danson, F., Ogunbadewa, E.Y., 2013. Probability of cloud-free observation conditions across Great Britain estimated using MODIS cloud mask. Remote Sens. Lett. 4, 427–435. https://doi.org/10.1080/2150704X.2012.744486.

Atzberger, C., Richter, K., 2012. Spatially constrained inversion of radiative transfer models for improved LAI mapping from future Sentinel-2 imagery. Remote Sens. Environ. 120, 208–218. https://doi.org/10.1016/j.rse.2011.10.035.

Atzberger, C., Richter, K., Vuolo, F., Darvishzadeh, R., Schlerf, M., 2011. Why confining to vegetation indices? Exploiting the potential of improved spectral observations using radiative transfer models. In: Proc. SPIE, pp. 81740Q. https://doi.org/10.1117/12.898479.

Atzberger, C., Darvishzadeh, R., Immitzer, M., Schlerf, M., Skidmore, A., le Maire, G., 2015. Comparative analysis of different retrieval methods for mapping grassland leaf area index using airborne imaging spectroscopy. Int. J. Appl. Earth Obs. Geoinf. 1–13. https://doi.org/10.1016/j.jag.2015.01.009.

Bégué, A., Arvor, D., Bellon, B., Betbeder, J., de Abelleyra, D., Ferraz, R.P.D., Lebourgeois, V., Lelong, C., Simões, M., Verón, S.R., 2018. Remote sensing and cropping practices: a review. Remote Sens. 10, 1–32. https://doi.org/10.3390/rs10010099.

Boschetti, M., Bocchi, S., Brivio, P.A., 2007. Assessment of pasture production in the Italian Alps using spectrometric and remote sensing information. Agric. Ecosyst. Environ. 118 (1-4), 267–272.

Bransby, D.I., Matches, A.G., Krause, G.F., 1977. Disk meter for rapid estimation of herbage yield in grazing Trials1. Agron. J. 69, 393–396.

Clevers, J.G.P.W., Gitelson, A.A., 2013. Remote estimation of crop and grass chlorophyll and nitrogen content using red-edge bands on Sentinel-2 and -3. Int. J. Appl. Earth Obs. Geoinf. 23, 344–351. https://doi.org/10.1016/j.jag.2012.10.008.

Danner, M., 2017. Retrieval of biophysical crop variables from multi-angular canopy spectroscopy. Remote Sens. 9, 726. https://doi.org/10.3390/rs9070726.

Darvishzadeh, R., Skidmore, A., Schlerf, M., Atzberger, C., 2008. Inversion of a radiative transfer model for estimating vegetation LAI and chlorophyll in a heterogeneous grassland. Remote Sens. Environ. 112, 2592–2604. https://doi.org/10.1016/j.rse.2007.12.003.

Darvishzadeh, R., Atzberger, C., Skidmore, A.K., Abkar, A.A., 2009. Leaf Area Index derivation from hyperspectral vegetation indices and the red edge position. Int. J. Remote Sens. 30, 6199–6218. https://doi.org/10.1080/01431160902842342.

Darvishzadeh, R., Atzberger, C., Skidmore, A., Schlerf, M., 2011. Mapping grassland leaf area index with airborne hyperspectral imagery: a comparison study of statistical approaches and inversion of radiative transfer models. ISPRS J. Photogramm. Remote Sens. 66, 894–906. https://doi.org/10.1016/j.isprsjprs.2011.09.013.

Delegido, J., Verrelst, J., Alonso, L., Moreno, J., 2011. Evaluation of sentinel-2 red-edge bands for empirical estimation of green LAI and chlorophyll content. Sensors 11, 7063–7081. https://doi.org/10.3390/s110707063.

Delegido, J., Verrelst, J., Meza, C.M., Rivera, J.P., Alonso, L., Moreno, J., 2013. A red-edge spectral index for remote sensing estimation of green LAI over agroecosystems. Eur. J. Agron. 46, 42–52. https://doi.org/10.1016/j.eja.2012.12.001.

Di Bella, C., Faivre, R., Ruget, F., Seguin, B., Guérif, M., Combal, B., Weiss, M., Rebella, C., 2004. Remote sensing capabilities to estimate pasture production in France. Int. J. Remote Sens. 25, 5359–5372. https://doi.org/10.1080/01431160410001719849.

Doktor, D., Lausch, A., Spengler, D., Thurner, M., 2014. Extraction of plant physiological status from hyperspectral signatures using machine learning methods. Remote Sens. https://doi.org/10.3390/rs61212247.

Dorigo, W.A., Zurita-Milla, R., de Wit, A.J.W., Brazile, J., Singh, R., Schaepman, M.E., 2007. A review on reflective remote sensing and data assimilation techniques for enhanced agroecosystem modeling. Int. J. Appl. Earth Obs. Geoinf. 9, 165–193. https://doi.org/10.1016/j.jag.2006.05.003.

Dorigo, W., Richter, R., Baret, F., Bamler, R., Wagner, W., 2009. Enhanced automated canopy characterization from hyperspectral data by a novel two step radiative transfer model inversion approach. Remote Sens. 1, 1139–1170. https://doi.org/10.3390/rs1041139.

Eastwood, C.R., Mata, G., Handcock, R., 2009. Evaluating satellite-based pasture measurement for Australian dairy farmers. In: Precision Livestock Farming. Proceedings of the Joint International Agriculture Conference. Wageningen, The Netherlands.

Edirisinghe, A., Clark, D., Waugh, D., 2012. Spatio-temporal modelling of biomass of intensively grazed perennial dairy pastures using multispectral remote sensing. Int. J. Appl. Earth Obs. Geoinf. 16, 5–16. https://doi.org/10.1016/j.jag.2011.11.006.

Fan, L., Gao, Y., Brück, H., Bernhofer, C., 2009. Investigating the relationship between NDVI and LAI in semi-arid grassland in Inner Mongolia using in-situ measurements. Theor. Appl. Climatol. 95, 151–156. https://doi.org/10.1007/s00704-007-0369-2.

Fava, F., Colombo, R., Bocchi, S., Meroni, M., Sitzia, M., Fois, N., Zucca, C., 2009. Identification of hyperspectral vegetation indices for Mediterranean pasture characterization. Int. J. Appl. Earth Obs. Geoinf. 11, 233–243. https://doi.org/10.1016/j.jag.2009.02.003.

Fernandes, R., Plummer, S.E., Nightingale, J., Baret, F., Camacho, F., Fang, H., Garrigues, S., Gobron, N., Lang, M., Lacaze, R., Leblanc, S., Meroni, M., Martinez, B., Nilson, T., Pinty, B., Pisek, J., Sonnentag, O., Verger, A., Welles, J., Weiss, M., Widlowski, J.-L., 2014. Global leaf area index product validation good practices. Version 2.0. In: Schaepman-Strub, Romain, M., Nickeson, J. (Eds.), Best Practice for Satelitte-derived Land Product Validation (p76): Land Product Validation Subgroup (WGCV/CEOS), pp. 1–78. https://doi.org/10.5067/doc/ceoswgcv/lpv/lai.002.

Ferraro, F.P., Nave, R.L.G., Sulc, R.M., Barker, D.J., 2012. Seasonal variation in the rising plate meter calibration for forage mass. Agron. J. 104, 1–6.

Frampton, W.J., Dash, J., Watmough, G., Milton, E.J., 2013. Evaluating the capabilities of Sentinel-2 for quantitative estimation of biophysical variables in vegetation. ISPRS J. Photogramm. Remote Sens. 82, 83–92. https://doi.org/10.1016/j.isprsjprs.2013.04.007.

Frederic, B., Buis, S., 2008. Estimating canopy characteristics from remote sensing observations: review of methods and associated problems. In: Liang, S. (Ed.), Advances in Land Remote Sensing. Springer-Verlag, Dordrecht, The Netherlands, pp. 173–201. https://doi.org/10.1007/978-1-4020-6450-0.

Gastellu-Etchegorry, J.P., Gascon, F., Estève, P., 2003. An interpolation procedure for generalizing a look-up table inversion method. Remote Sens. Environ. 87, 55–71. https://doi.org/10.1016/S0034-4257(03)00146-9.

Gowda, P.H., Oommen, T., Howell, T.H., Schartz, R., 2016. Retrieving leaf area index from remotely sensed data using advanced statistical approaches. J. Remote Sens. GIS 5 (156), 1–6. https://doi.org/10.4172/2469-4134.1000156.

Handcock, R.N., Mata, G., Gherardi, S.G., 2008. Combining spectral information aggregated to the paddock scale with knowledge of on-farm practices will enhance remote sensing methods for intensively managed dairy pastures. In: 14th Australian Remote Sensing & Photogrammetry Conference. Darwin, Australia, pp. 1–10.

Herrmann, I., Pimstein, A., Karnieli, A., Cohen, Y., Alchanatis, V., Bonfil, D.J., 2011. LAI assessment of wheat and potato crops by VENμS and Sentinel-2 bands. Remote Sens. Environ. 115, 2141–2151. https://doi.org/10.1016/j.rse.2011.04.018.

Hill, M.J., Donald, G.E., Hyder, M.W., Smith, R.C.G., 2004. Estimation of pasture growth rate in the south west of Western Australia from AVHRR NDVI and climate data. Remote Sens. Environ. 93, 528–545. https://doi.org/10.1016/j.rse.2004.08.006.

Houborg, R., Soegaard, H., Boegh, E., 2007. Combining vegetation index and model inversion methods for the extraction of key vegetation biophysical parameters using Terra and Aqua MODIS reflectance data. Remote Sens. Environ. 106, 39–58. https://doi.org/10.1016/j.rse.2006.07.016.

Huillier, P.J.L., Thomson, N.A., 1988. Estimation of herbage mass in ryegrass/white clover dairy pastures. Proc. New Zeal. Grassl. Assoc. 49, 117–122.

Jacquemoud, S., Baret, F., 1990. PROSPECT: a model of leaf optical properties spectra. Remote Sens. Environ. 34, 75–91. https://doi.org/10.1016/0034-4257(90)90100-Z.
Jacquemoud, S., Verhoef, W., Baret, F., Bacour, C., Zarco-Tejada, P.J., Asner, G.P., François, C., Ustin, S.L., 2009. PROSPECT + SAIL models: a review of use for vegetation characterization. Remote Sens. Environ. 113, S56–S66. https://doi.org/10.1016/j.rse.2008.01.026.
Jin, Y., Yang, X., Qiu, J., Li, J., Gao, T., Wu, Q., Zhao, F., Ma, H., Yu, H., Xu, B., 2014. Remote sensing-based biomass estimation and its spatio-temporal variations in temperate Grassland, northern China. Remote Sens. 6, 1496–1513. https://doi.org/10.3390/rs6021496.
Kemp, P.D., Kenyon, P.R., Morris, S.T., 2010. The use of legume and herb forage species to create high performance pastures for sheep and cattle grazing systems. Rev. Bras. Zootec. 39, 169–174.
Li, Z., Wang, J., Tang, H., Huang, C., Yang, F., Chen, B., Wang, X., Xin, X., Ge, Y., 2016. Predicting grassland leaf area index in the meadow steppes of northern China: a comparative study of regression approaches and hybrid geostatistical methods. Remote Sens. 8. https://doi.org/10.3390/rs8080632.
Maclellan, C., 2017. Dual FOV Measurements With SVC HR-1024i Field Spectroradiometers – Bi-conical Relative Reflectance Method. (Edinburgh, UK).
Mata, G., Purdie, N., Handcock, R.N., Dalley, D., Ota, N., Rossi, L., 2011. Validating satellite monitoring of dairy pastures in Canterbury with Lincoln University Dairy Farm and commercial farm data. In: Proceedings of the New Zealand Grassland Association 73, pp. 109–114 (New Zealand).
Meng, B., Liang, T., Ge, J., Gao, J., Yin, J., 2017. Evaluation of above ground biomass estimation accuracy for alpine meadow based on MODIS vegetation indices 2 data and methods. In: ITM Web of Conferences. 12. pp. 0–5.
Mutanga, O., Skidmore, A.K., 2004. Integrating imaging spectroscopy and neural networks to map grass quality in the Kruger National Park, South Africa. Remote Sens. Environ. 90, 104–115. https://doi.org/10.1016/j.rse.2003.12.004.
Myneni, R.B., Knyazikhin, Y., Privette, J.L., Running, S.W., Nemani, R., Zhang, Y., Tian, Y., Wang, Y., Morissette, J.T., Glassy, J., Votava, P., 1999. MODIS Leaf Area Index (LAI) and Fraction of Photosynthetically Active Radiation Absorbed By Vegetation (FPAR) Product. Modis Atbd Version 4. 130. http://eospso.gsfc.nasa.gov/atbd/modistables.html.
Nakagami, K., Itano, S., 2013. Improving pooled calibration of a rising-plate meter for estimating herbage mass over a season in cool-season grass pasture. Grass Forage Sci. 69, 717–723. https://doi.org/10.1111/gfs.12070.
Olioso, A., Inoue, Y., Demarty, J., 2005. Olioso_Future Directions for Advaced Evapotranspiration Modeling Assimilation of Remote Sensing Data Into Crop Simulation Models and Svat Models.pdf. pp. 377–412.
Ozdogan, M., Yang, Y., Allez, G., Cervantes, C., 2010. Remote sensing of irrigated agriculture: opportunities and challenges. Remote Sens. 2, 2274–2304. https://doi.org/10.3390/rs2092274.
Pullanagari, R.R., Kereszturi, G., Yule, I.J., 2016. Mapping of macro and micro nutrients of mixed pastures using airborne AisaFENIX hyperspectral imagery. ISPRS J. Photogramm. Remote Sens. 117, 1–10. https://doi.org/10.1016/j.isprsjprs.2016.03.010.
Pullanagari, R.R., Kereszturi, G., Yule, I.J., 2017. Quantification of dead vegetation fraction in mixed pastures using AisaFENIX imaging spectroscopy data. Int. J. Appl. Earth Obs. Geoinf. 58, 26–35. https://doi.org/10.1016/j.jag.2017.01.004.
Punalekar, S., Verhoef, A., Tatarenko, I., van der Tol, C., MacDonald, D., Marchant, B., Gerard, F., White, K., Gowing, D., 2016. Characterization of a highly biodiverse floodplain meadow using hyperspectral remote sensing within a plant functional trait framework. Remote Sens. 8, 112. https://doi.org/10.3390/rs8020112.
Richter, K., Hank, T.B., Vuolo, F., Mauser, W., D'Urso, G., 2012. Optimal exploitation of the sentinel-2 spectral capabilities for crop leaf area index mapping. Remote Sens. 4, 561–582. https://doi.org/10.3390/rs4030561.
Rivera, J.P., Verrelst, J., Leonenko, G., Moreno, J., 2013. Multiple cost functions and regularization options for improved retrieval of leaf chlorophyll content and LAI through inversion of the PROSAIL model. Remote Sens. 5, 3280–3304. https://doi.org/10.3390/rs5073280.
Schino, G., Borfecchia, F., Cecco, L. De, Dibari, C., Iannetta, M., Martini, S., Pedrotti, F., Protezione, U.T.S.B., Casaccia, C.R., Speciale, P., Globale, C., 2003. Satellite estimate of grass biomass in a mountainous range in Central Italy. Agrofor. Syst. 59, 157–162.
Schucknecht, A., Meroni, M., Kayitakire, F., Boureima, A., 2017. Phenology-based biomass estimation to support rangeland management in semi-arid environments. Remote Sens. 9. https://doi.org/10.3390/rs9050463.
Sibanda, M., Mutanga, O., Rouget, M., 2015. Examining the potential of Sentinel-2 MSI spectral resolution in quantifying above ground biomass across different fertilizer treatments. ISPRS J. Photogramm. Remote Sens. 110, 55–65. https://doi.org/10.1016/j.isprsjprs.2015.10.005.
Sleugh, B., Moore, K.J., George, J.R., Brummer, E.C., 2000. Binary legume–grass mixtures improve forage yield, quality, and seasonal distribution journal paper no. J-18184 of the Iowa Agric. and Home Econ. Exp. Stn., Ames, IA, Project No. 2899, and supported by Hatch Act and State of Iowa funds. Agron. J. 92, 24–29. https://doi.org/10.2134/agronj2000.92124x.
Somasiri, S.C., Kenyon, P.R., Morel, P.C.H., Kemp, P.D., Morris, S.T., 2014. Alternative method to measure herbage dry matter mass in plantain and chicory mixed swards grazed by lambs. In: Proceedings of the New Zealand Society of Animal Production, pp. 115–120.
Song, W., Jia, H., Liu, S., Liang, S., Wang, Z., Hao, L., Chai, S., 2014. A remote sensing based forage biomass yield inversion model of alpine-cold meadow during grass-withering period in Sanjiangyuan area. IOP Conf. Ser. Earth Environ. Sci. 17, 8–14. https://doi.org/10.1088/1755-1315/17/1/012042.
Thomson, N.A., McCallum, D.A., Howse, S., Holmes, C.W., Matthews, P.N.P., 1997. Estimation of Dairy Pastures – The Need for Standardisation. 225. pp. 221–225.
Thornton, P.K., 2010. Livestock production: recent trends, future prospects. Philos. Trans. R. Soc. Lond. Ser. B Biol. Sci. 365, 2853–2867. https://doi.org/10.1098/rstb.2010.0134.
Verhoef, W., 1984. Light scattering by leaf layers with application to canopy reflectance modeling: the SAIL model. Remote Sens. Environ. 16, 125–141. https://doi.org/10.1016/0034-4257(84)90057-9.
Verhoef, W., 1998. Theory of Radiative Transfer Models Applied in Optical Remote Sensing of Vegetation Canopies. Wageningen Agricultural University.
Verhoef, W., Bach, H., 2007. Coupled soil-leaf-canopy and atmosphere radiative transfer modeling to simulate hyperspectral multi-angular surface reflectance and TOA radiance data. Remote Sens. Environ. 109, 166–182. https://doi.org/10.1016/j.rse.2006.12.013.
Verhoef, W., van der Tol, C., Middleton, E.M., 2018. Hyperspectral radiative transfer modeling to explore the combined retrieval of biophysical parameters and canopy fluorescence from FLEX – Sentinel-3 tandem mission multi-sensor data. Remote Sens. Environ. 204, 942–963. https://doi.org/10.1016/j.rse.2017.08.006.
Verrelst, J., Rivera, J.P., Leonenko, G., Alonso, L., Moreno, J., 2014. Optimizing LUT-based RTM inversion for semiautomatic mapping of crop biophysical parameters from sentinel-2 and -3 data: role of cost functions. IEEE Trans. Geosci. Remote Sens. 52, 257–269. https://doi.org/10.1109/TGRS.2013.2238242.
Verrelst, J., Camps-Valls, G., Muñoz-Marí, J., Rivera, J.P., Veroustraete, F., Clevers, J.G.P.W., Moreno, J., 2015. Optical remote sensing and the retrieval of terrestrial vegetation bio-geophysical properties - a review. ISPRS J. Photogramm. Remote Sens. 108, 273–290. https://doi.org/10.1016/j.isprsjprs.2015.05.005.
Vohland, M., Jarmer, T., 2008. Estimating structural and biochemical parameters for grassland from spectroradiometer data by radiative transfer modelling (PROSPECT + SAIL). Int. J. Remote Sens. 29, 191–209. https://doi.org/10.1080/01431160701268947.
Vohland, M., Mader, S., Dorigo, W., 2010. Applying different inversion techniques to retrieve stand variables of summer barley with PROSPECT + SAIL. Int. J. Appl. Earth Obs. Geoinf. 12, 71–80. https://doi.org/10.1016/j.jag.2009.10.005.
Weiss, M., Baret, F., Myneni, R.B., Pragnere, A., Knyazikhin, Y., 2000. Investigation of a model inversion technique to estimate canopy biophysical variables from spectral and directional reflectance data. Agronomie 20, 3–22. https://doi.org/10.1051/agro:2000105.
Wilcox, C., Strout, M.M., Bieman, J.M., 2011. Tool support for software lookup table optimization. Sci. Program. 19, 213–229. https://doi.org/10.1155/2011/813675.
Woodward, S.L., Waugh, C.D., Roach, C.G., Fynn, D., Phillips, J., 2013. Are diverse species mixtures better pastures for dairy farming? Proc. New Zeal. Grassl. Assoc. 75, 79–84.
Zhao, F., Xu, B., Yang, X., Jin, Y., Li, J., Xia, L., Chen, S., Ma, H., 2014. Remote sensing estimates of grassland aboveground biomass based on MODIS Net Primary Productivity (NPP): a case study in the Xilingol Grassland of northern China. Remote Sens. 6, 5368–5386. https://doi.org/10.3390/rs6065368.